Conformational Analysis with Both Experimental and Computational Data for Both Gaseous and Crystalline Phases: Unexpected Interactions in *N*-Methyldichloroacetamide

Sarah L. Hinchley,[†] Heather E. Robertson,[†] Lorna J. McLachlan,[†] Carole A. Morrison,[†] David W. H. Rankin,*[,†] Stephen J. Simpson,[‡] and Emrys W. Thomas[§]

School of Chemistry, University of Edinburgh, West Mains Road, Edinburgh, EH9 3JJ, United Kingdom, Chemistry Department, School of Sciences, University of Salford, Salford, Greater Manchester, M5 4WT, United Kingdom, and Division of Biological Sciences, School of Environment and Life Sciences, University of Salford, Salford, Greater Manchester, M5 4WT, United Kingdom

Received: August 20, 2003; In Final Form: November 6, 2003

The structure of *N*-methyldichloroacetamide ($MeNHCOCHCl_2$) has been elucidated in the gaseous and solid states experimentally by gas electron diffraction and X-ray crystallography, and computationally with ab initio and plane-wave DFT methods. Although the main structural parameters generally agree well, the orientation of the $CHCl_2$ group relative to the carbonyl oxygen was found to be very different in the solid and gas phases. X-ray crystallography and solid-state plane-wave DFT methods indicate that the bond torsion angle ϕ(HCCO) is 180.0°, while ab initio and gas electron diffraction methods return ϕ(HCCO) as −13.1° and −31.8(22)°, respectively. Further investigation of this phenomenon was carried out by using various computational methods. The possibility of intermolecular H···O and Cl···O bonds, which would stabilize the solid-state structure, was investigated by both solid-state plane-wave DFT and single-point ab initio methods. Ab initio SCRF calculations were also employed to evaluate solvent effects on the structure, using the Onsager reaction field model.

Introduction

Rotational isomerism in several α-halo-substituted acetic acids and their derivatives has been intensively studied by ab initio, spectroscopic, and diffraction methods.[1−6] With regard to 2,2-dichloroacetic acid,[7] its methyl ester,[8] and acyl chloride,[9] several studies indicate clearly the presence of two low-energy conformers derived from rotational isomerism of the dichloromethyl group. They are syn conformers in which the HCCO torsion angle is ∼0°, and gauche conformers in which this torsion angle is ∼140° (with eclipsing of Cl and O atoms). A slight preference for the syn form is shown, particularly for the ester and acyl chloride. With regard to the *N*-methylamide of dichloroacetic acid, however, the available evidence (based on an IR study) indicates the presence of just one conformer in dilute tetrachloromethane solution, with stabilization of another conformer in the presence of added H-bond acceptors.[10] As chloramphenicol, an important antibiotic drug, contains the $-NHCOCHCl_2$ moiety, understanding of the conformations of such species, as free molecules, in solution, and in the solid phase, is important. In the absence of definitive structural data on this particular amide, a combined gas-phase electron diffraction, X-ray diffraction, and ab initio study has been undertaken to determine conformational preferences of the dichloromethyl group. This work complements a parallel modeling study[11] of the solution conformation of chloramphenicol.

Experimental Section

Synthesis. *N*-Methyldichloroacetamide (melting point 348 K, lit. mp 346−348 K) was prepared according to literature methods[12] by aminolysis of ethyl dichloroacetate in 30% w/v aqueous methylamine, followed by double re-crystallization from diethyl ether. A sample was provided for use in the gas electron diffraction apparatus without further purification.

Theoretical Methods. All geometry optimization and frequency calculations were performed on a dual-processor Pentium III 1000-MHz workstation with the Gaussian 98program.[13] The MP2/6-311++G** force-field calculations were performed with resources of the EPSRC National Service for Computational Chemistry Software, on a cluster of 6 HP ES40 computers. Each Alphaserver ES40 machine has four 833 MHz EV68 CPUs and 8 GB of memory. All MP2 calculations were frozen core [MP2(fc)]. The solvation calculations were performed on a single-processor NT Pentium 4 1.5 GHz workstation. Plane-wave DFT calculations were carried out with CASTEP version 2.2[14]on a Linux 800 MHz dual-processor PC.

Geometry Optimizations. An extensive search of the torsional potential of $MeNHCOCHCl_2$ was undertaken at the HF/3-21G*[15−17] level to locate all minima. Two different orientations of the N−C(O) bond were investigated, syn with ϕ(CNCO) = 0° and anti with ϕ(CNCO) = 180°. For each of these conformers, four possible orientations of the $CHCl_2$ group relative to the carbonyl oxygen were investigated, giving ϕ(HCCO) = 0°, 60°, 120°, and 180°. This gives eight possible structures: *syn0*, *syn60*, *syn120*, *syn180*, *anti0*, *anti60*, *anti120*, and *anti180*. For the syn structures investigated, two conformers, *syn0* and *syn120*, were found. For the anti structures (ϕ(CNCO) = 180°), two conformers were also located, *anti0* and *anti120*. For both the syn and anti conformers, the structures were of C_1 symmetry due to nonplanarity at the nitrogen atom, but one (*anti120*) was very close to C_s symmetry. Further geometry optimizations were undertaken for all the conformers at the HF and MP2 levels with the standard 6-31G*[18−20] basis set, and at

* Address correspondence to this author. E-mail: d.rankin@ed.ac.uk.
† School of Chemistry, University of Edinburgh.
‡ School of Sciences, University of Salford.
§ School of Environment and Life Sciences, University of Salford.

10.1021/jp036478h CCC: $27.50
Published on Web 12/10/2003

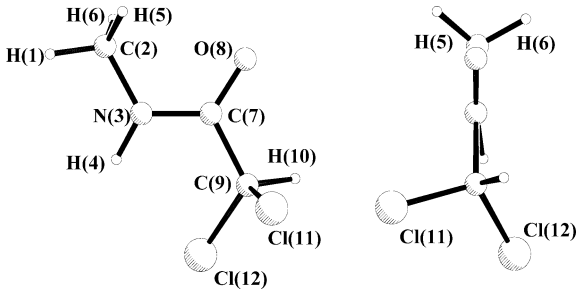

Figure 1. Molecular structure of $MeNHCOCHCl_2$ showing (a) a perspective view and (b) a view along the C(7)−N(3) bond.

the MP2 level with the 6-311G*,[21,22] 6-311+G*, and 6-311++G** basis sets. The lowest energy structure of $MeNHCOCHCl_2$ and the atom numbering scheme are shown in Figure 1.

Frequency Calculations. Numeric second derivatives of the energy with respect to nuclear coordinates calculated at the MP2/6-311++G** level for $MeNHCOCHCl_2$ gave the force field. This was used to provide estimates of the amplitudes of vibration (u) and the curvilinear corrections (k) for use in the gas electron diffraction (GED) refinements. This improved level of theory and large basis set were used for the force-field calculation, because a large change in ϕ(HCCO) was observed on the inclusion of diffuse functions. The analytic force fields calculated at the HF/6-31G* level were used to calculate the frequencies for all the optimized structures, which in turn provided information about the nature of stationary points.

Solvation Calculations. Self-consistent reaction field calculations were performed at the B3LYP/6-31G** level[23] with use of the Onsager model.[24] Two different solvent systems were investigated: tetrachloromethane (TCM) and dimethyl sulfoxide (DMSO). The solute was set to occupy a fixed spherical cavity of radius $a_0 = 407$ pm for both TCM and DMSO within the solvent field. Dielectric constants of $\epsilon = 2.23$ and 46.7 were used for TCM and DMSO, respectively. In this model the molecular dipole interacts with the dielectric continuum, leading to a net stabilization that should be observable for each solvent system. A full potential search of the bond torsion ϕ(HCCO) at 20° intervals (0° to 360°) was performed for both tetrachloromethane and dimethyl sulfoxide.

Single-Point Energy Calculations. The crystal structure coordinates were used for ab initio molecular orbital (ab initio MO) single-point energy calculations to evaluate ab initio the strengths of the interactions within the solid-state structure. A monomer of *N*-methyldichloroacetamide and two dimers with different interactions were calculated with two different methods, MP2/6-311++G** and PW91PW91/6-311++G**. The strengths of the interactions would be overestimated by both MP2 and DFT methods unless Basis Set Superposition Error (BSSE) was corrected for. This was done by using the Counterpoise (CP) correction.[25] The first dimer investigated showed interlayer Cl···O bonding (Figure 2a), and the second displayed two intralayer H···O bonds (Figure 2b).

Plane-Wave DFT Calculations. A series of plane-wave DFT (PW-DFT) calculations were carried out on *N*-methyldichloroacetamide to investigate further the strengths of the interactions between the molecules in the solid phase. A generalized gradient approximation (GGA-PBE) was used for the exchange and correlation potential.[26] The wave function was generated by using a series of pseudopotentials and delocalized plane waves expressed at an energy cutoff of 300 eV.

Crystal Lattice Calculation. This calculation used the lattice vectors and atomic coordinates from the low-temperature crystal

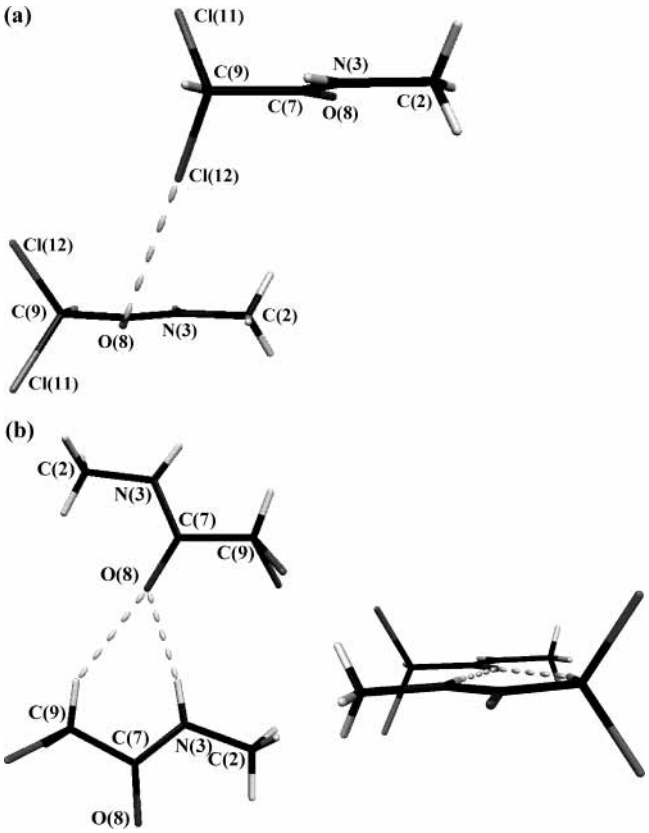

Figure 2. Solid-state dimer models used for the ab initio MO single point energy calculations of (a) the interlayer Cl···O interaction and (b) the intralayer H···O interactions.

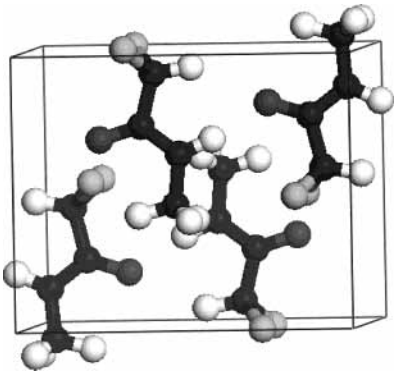

Figure 3. X-ray crystallographic structure of *N*-methyldichloroacetamide.

structure reported later in this paper. The unit cell volume and atom positions were allowed to optimize until convergence was achieved (changes in energy per atom to within 2.0×10^{-5} eV and forces within 0.05 eV $Å^{-1}$). The symmetry-reduced k-point sets used to sample the reciprocal space were generated by using Monkhurst−Pack grids[27] (dimensions $2 \times 2 \times 3$, giving 2 k-points in the symmetry-reduced first Brillouin zone). A diagram of the unit cell is given in Figure 3.

Supercell Calculations. These two calculations involved an isolated molecule of *N*-methyldichloroacetamide in a $1200 \times 1200 \times 1200$ pm^3 unit cell, the first being a single-point energy calculation, the second being a geometry optimization. The purpose of the periodic (PW-DFT) calculation was to investigate the properties of the intermolecular interactions within a periodic environment to contrast with results obtained from the ab initio MO single-point calculations. The starting geometry for the isolated molecule was taken from the optimized geometry of

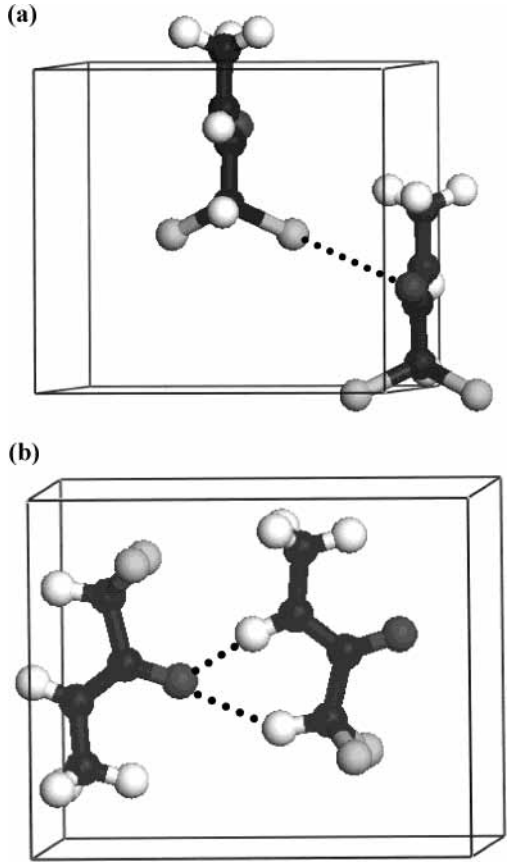

Figure 4. Solid-state dimer models used for the PW-DFT calculations of (a) the Cl···O interaction and (b) the H···O interactions.

the first calculation. The same energy cutoff and convergence criteria were used as in the crystal lattice. Integrations over the symmetrized Brillouin zone were performed using one *k*-point positioned at the Γ-point.

H···O and Cl···O Interactions. Calculations were carried out to determine the strengths of the two types of interactions, namely the combined strength of the hydrogen bonds and the Cl···O interaction. In the two models, two molecules were removed from the unit cell to destroy the hydrogen bonds in the first calculation and the Cl···O interaction in the second [see Figure 4, panels a and b]. The energies of the interactions were obtained by comparing the energy per molecule from these calculations with those from the optimized crystal lattice calculation. A cutoff energy of 300 eV was used, the same as for the supercell and crystal lattice calculations to allow comparison, and *k*-point sampling grids of $2 \times 3 \times 2$.

Electron Diffraction Measurements. Data were collected with the Edinburgh gas diffraction apparatus.[28] An accelerating voltage of ca. 40.0 kV (electron wavelength ca. 6.0 pm) was used, while maintaining the sample and nozzle temperatures at 403 and 410 K, respectively. Scattering intensities were recorded at nozzle-to-plate distances of 98 and 252 mm on Kodak Electron Image films. The weighting points for the off-diagonal weight matrixes, correlation parameters, and scale factors for the two camera distances are given in Table S1 (Supporting Information), together with electron wavelengths, which were determined from the scattering patterns of benzene vapor, recorded immediately after the compound patterns and analysed in exactly the same way to minimize systematic errors in wavelengths and camera distances. The electron-scattering patterns were converted into digital form by using a PDS densitometer at the Institute of Astronomy, Cambridge University, UK with a scanning program described elsewhere.[29] Data reduction and least-squares refinements were carried out with standard programs,[30,31] employing the scattering factors of Ross et al.[32]

X-ray Diffraction Measurements. A suitable crystal was mounted on a glass fiber with epoxy resin and cooled in a stream of nitrogen gas on a Siemens P4 diffractometer. Careful centering of 29 reflections in the 2θ range $10-25°$ gave a unit cell. Data were collected with use of variable scan rates with three check reflections monitored every 100 reflections. Programs XSCHNS and SHELXL were used for data collection and refinement. Atomic coordinates and thermal parameters have been deposited at the Cambridge Crystallographic Database. Details of data collection for $MeNHCOCHCl_2$ are given in Table S2 of the Supporting Information.

Results

Theoretical Methods. The eight possible structures of $MeNHCOCHCl_2$ described previously in the Experimental Section were investigated ab initio. Of the four syn conformers studied, only two were returned as minima on the potential energy surface at the HF/6-31G* level. It was observed that *syn180* collapsed to the same structure as *syn120* with ϕ(HCCO) $= 118°$, and *syn60* collapsed to the *syn0* structure with ϕ(HCCO) $= 0°$. The lowest lying frequency for *syn120* was just 15 cm^{-1}, and this motion is associated with the HCCO torsion, compared to the next frequency of 104 cm^{-1} (methyl torsion). For *syn0*, the lowest lying frequency was 25 cm^{-1} for the HCCO bond torsion, with one at 32 cm^{-1} (methyl torsion). At the HF/6-31G* level, *syn120* was found to be 11.7 kJ mol^{-1} less stable than *syn0*. *Syn120* and *syn0* were both taken to a higher level of theory with the same basis set (MP2/6-31G*), at which point both returned the *syn0* structure. From this we concluded that there is only one syn conformer, with ϕ(HCCO) $\approx 0°$.

The anti conformers were investigated in the same manner as the syn ones. At the HF/6-31G* level two conformers, *anti0* and *anti120*, were minima on the potential energy surface, with *anti60* and *anti180* collapsing back to *anti0* and *anti120*, respectively, as in the syn case. ϕ(HCCO) was 3° for *anti0* and 149° for *anti120*. At the MP2/6-31G* level, both conformers were returned. A summary of ϕ(CNCO), ϕ(HCCO), and molecular energies at the HF/6-31G* and MP2/6-311++G** levels for all four conformers is given in Table 1. The molecular geometry of the lowest energy conformer of $MeNHCOCHCl_2$ at the MP2/6-311++G** level (*syn0*) is given in Table 2. The molecular geometries calculated at the HF/6-31G*, MP2/6-31G*, MP2/6-311G*, MP2/6-311+G*, and MP2/6-311++G** levels to compare the effects of improving basis set and level of theory and the effect of inclusion of polarization and diffuse functions on the structural parameters are given in Table S3 in the Supporting Information.

At the highest level of theory and basis set investigated (MP2/6-311++G**), the anti conformers were at least 15 kJ mol^{-1} higher in energy than the syn conformer. At room temperature an energy difference of 15 kJ mol^{-1} would correspond to 99.7% of the lower energy conformer and 0.3% of the higher energy conformer being observed in the gas-phase electron diffraction experiment. The tiny amount of the higher energy conformer would be undetectable in the GED experiment. Thus the results of the ab initio calculations for the *syn0* structure will be the only ones analyzed here unless otherwise stated.

The C−N bond associated with the sp^3 carbon [C(2)−N(3)] varies little with increased level of theory and bigger basis set. However, the C−N bond with the sp^2 carbon [C(7)−N(3)]

TABLE 1: Comparison of Energies for the Four Conformers of $MeNHCOCHCl_2$ (all C_1) at the HF/6-31G* and MP2/6-311++G Levels and Torsion Angles ϕ(CNCO) and ϕ(HCCO)[a,b]**

level of theory	parameter	*syn0*	*syn120*	*anti0*	*anti120*
HF/6-31G*	energy[c]	−1164.8827	−1164.8784	−1164.8754	−1164.8727
	ϕ(CNCO)	0.1	7.1	−173.3	−179.7
	ϕ(HCCO)	−0.1	118.1	2.6	149.4
	ΔE[e]	0.0	+11.3	+19.2	+26.3
MP2/6-311++G**	energy[d]	−1166.0029		−1165.9972	−1165.9942
	ϕ(CNCO)	3.1		−169.6	178.4
	ϕ(HCCO)	−13.1		1.62	150.5
	ΔE[e]	0.0		+15.0	+22.8

[a] See text for conformer definitions. [b] Energies in hartrees. [c] Corrected for zero point energy. [d] Not corrected for zero point energy. [e] Energy in kJ mol^{-1}.

TABLE 2: Refined and Calculated Geometric Parameters for $MeNHCOCHCl_2$ (distances in pm, angles in deg) from the GED Study[a,b]

no.	parameter	MP2/6-311++G** (r_e)	GED (r_{h1})	restraint
		independent parameters		
p_1	(C−H mean + N−H)/2	105.1	105.1(4)	105.1(5)
p_2	C−H mean − N−H	8.3	8.4(6)	8.3(5)
p_3	[C(7)−C(9) + C(7)−N(3) + C(2)−N(3)]/3	144.6	145.8(2)	144.6(4)
p_4	C−C − [(C(7)−N + C(2)−N)/2]	13.1	11.9(4)	13.1(4)
p_5	C(2)−N(3) − C(7)−N(3)	10.3	9.9(4)	10.3(4)
p_6	C═O	122.4	124.7(3)	
p_7	C−Cl mean	177.7	178.4(2)	
p_8	H−C−H mean	109.1	107.6(10)	109.1(10)
p_9	C(2)−N(3)−C(7)	120.3	118.7(10)	120.3(18)
p_{10}	H(4)−N(3)−C(7)	119.0	118.9(8)	119.0(7)
p_{11}	N(3)−C(7)═O(8)	124.4	123.0(4)	
p_{12}	N(3)−C(7)−C(9)	115.9	118.0(6)	
p_{13}	C(7)−C(9)−H(10)	107.4	107.4(4)	107.4(3)
p_{14}	Cl(11)−C(9)−Cl(12)	111.4	110.7(2)	
p_{15}	H(10)−C(9)−Cl(11)	108.1	108.0(12)	108.1(10)
p_{16}	[C(7)−C(9)-Cl(11) + C(7)−C(9)−Cl(12)]/2	110.9	112.7(2)	
p_{17}	C(7)−C(9)−Cl(11) − C(7)−C(9)−Cl(12)	2.1	4.1(9)	2.1(10)
p_{18}	O(8)═C(7)−C(9)−H(10)	−13.1	−31.8(22)	
p_{19}	H(1)−C(2)−N(3)−C(7) (methyl torsion)	−173.0	−173.1(24)	−173.0(20)
p_{20}	C(2)−N(3)−C(7)═O(8)	3.1	2.0(24)	3.1(31)
p_{21}	H dip	10.7	10.5(24)	10.7(20)
		dependent parameters		
p_{22}	N(3)−C(7)	135.1	136.9(3)	
p_{23}	C(2)−N(3)	145.4	146.8(3)	
p_{24}	C(7)−C(9)	153.3	153.7(3)	
p_{25}	N(3)−H(4)	100.9	100.9(5)	
p_{26}	C(2)−N(3)−H(4)	119.8	121.5(13)	
p_{27}	O(8)═C(7)−C(9)	119.4	119.0(6)	
p_{28}	C(7)−C(9)−Cl(11)	112.0	110.7(5)	
p_{29}	C(7)−C(9)−Cl(12)	109.9	114.7(5)	

[a] Numbers in parentheses are the estimated standard deviations of the last digits. [b] See text for parameter definitions.

lengthens by 1.5 pm on increasing the level of theory, decreases by 3 pm on going from a double-ζ to triple-ζ basis set, then lengthens by 2.9 pm on the inclusion of diffuse functions (6-311+G*). Whereas we can say that C(2)−N(3) has converged with respect to basis set and level of theory, i.e., its value changes little on improving both, we cannot say this for the C(7)−N(3) bond length, which fluctuates wildly. Having observed this fluctuation for the C(7)−N(3) bond length, it is interesting to observe the C(7)−O(8) bond length behavior. The inclusion of electron correlation has a large effect on this distance, as expected (HF/6-31G* = 119.6 pm, MP2/6-31G* = 123.1 pm). Improving the basis set to triple-ζ reduces the bond length by 1 pm to 122.1 pm, and the inclusion of diffuse functions does not affect the parameter much (0.3 pm longer). Thus the C−O bond appears to be reaching convergence, whereas the C−N bond does not. Another unexpected feature is the lack of sensitivity of the C−Cl bonds to the inclusion of electron correlation and improvement of basis set. The biggest variation by either bond is 0.3 pm, whereas we expected a much bigger change upon the inclusion of electron correlation and diffuse functions.

Although the C−Cl bond distances are seemingly unaffected by changes in basis set and level of theory for this molecule, the C−C−Cl bond angles are slightly affected, mainly upon the inclusion of diffuse functions. Here, a decrease of 1.3° is observed for C(7)−C(9)−Cl(11), while an increase of 0.9° is observed for C(7)−C(9)−Cl(12). The Cl−C−Cl angle remains very stable, varying little upon the inclusion of electron correlation or change in basis set. The bond angles around N(3) differ by as much as 3.4° (MP2/6-31G*) but N(3) is calculated to be planar in all but the 6-311+G* and 6-311++G** cases. At the MP2/6-311+G* level the sum of the angles around N(3) is 359.7°, indicating only a very slight deviation from planarity at nitrogen, and at the MP2/6-311++G** level the sum is 359.1°. The range of angles at the MP2/6-311+G* level is the smallest (120.3−119.6°; 0.7°). A much wider range of bond angles is observed about C(7), with the largest at the MP2/6-311G* level (125.8−115.2°; 10.6°). Again the carbonyl carbon

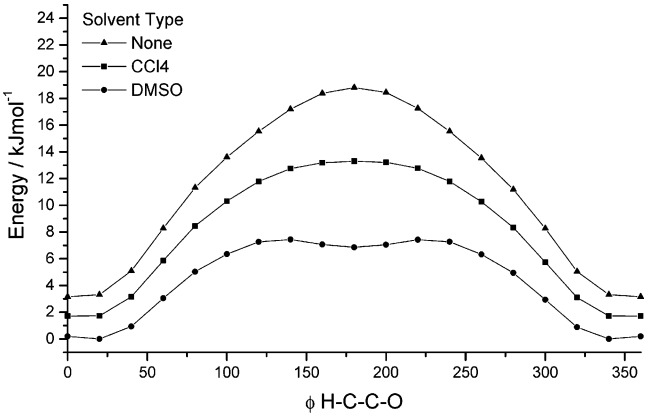

Figure 5. Effect of various solvents on the fluid-phase structure of *N*-methyldichloroacetamide.

is returned as planar at all levels except MP2/6-311++G**, and even in this case the sum of angles around C(7) is 359.7°, individual angles ranging from 124.4° [N(3)−C(7)−O(8)] to 115.9° [N(3)−C(7)−C(9)]. The H−C−H angles are also unaffected by the change in basis set and level of theory, and are hardly distorted from the perfect tetrahedral angle of 109.5° (109.1°, MP2/6-311++G**). This indicates that the methyl group is not distorted by either steric or electronic effects.

One parameter that does vary wildly with the inclusion of electron correlation, the increase in basis set size, and functionality is the bond torsion about C(7)−C(9). ϕ(HCCO) changes from −0.1° to −5.2° upon the inclusion of electron correlation with the 6-31G* basis set. The bond torsion then changes to 0.2° when the basis set is increased to 6-311G*. The most dramatic effect is seen upon the inclusion of diffuse functions, when ϕ(HCCO) changes from 0.2° to −13.1°, a change of 13.3°. ϕ(CNCO) does not vary so much on including electron correlation, or with increased basis set size. However, on going from a 6-311+G* basis set to a 6-311++G** basis set, a 2.1° increase is observed. Along with the slightly pyramidal nature of the nitrogen, this serves to remove the planarity of the CN(H)C(O)C backbone of the molecule.

Solvent Effect Calculations. It was observed that the orientation of the $CHCl_2$ group relative to the carbonyl group was very different between the solid and gaseous structures. One of the techniques used to try to account for this different orientation was solvation modeling. The conformation observed in the solid state is relatively polar and could in principle originate from a similar conformer preferentially stabilized in the polar media used during the synthesis of the amide. A full potential energy surface scan of the ϕ(HCCO) bond torsion was performed at the B3LYP/6-31G** level with tetrachloromethane and dimethyl sulfoxide as solvents. The results (Figure 5) indicate that the most stable conformer of *N*-methyldichloroacetamide has ϕ(HCCO) between −20° and 20° in the media studied. The calculations in DMSO, however, show stabilization of a higher energy conformer with ϕ(HCCO) ∼ 180°. This conformer is calculated to be 6.9 kJ mol^{-1} higher in energy than the global minimum at the B3LYP/6-31G** level, corresponding to a 94.2:5.8 mixture of conformers at room temperature. On this basis solvent stabilization seems to be an unlikely explanation for the $CHCl_2$ rotameric state in the solid. It is also worth noting the absence of solvent molecules in the crystal structure itself.

Single-Point Energy Calculations. The results of the ab initio MO single-point energy (MP2 and DFT) calculations for the monomer and two dimers of the solid-state structure are given in Table 3. All energies quoted hereafter are those corrected for BSSE by using the CP correction. Solid-state calculations, as they are plane wave in nature, do not account for dispersion forces in long-range interactions. By using the exchange component and the gradient-corrected correlation functional of Perdew and Wang for the ab initio MO DFT calculation and comparing the results to the MP2 calculations, we can evaluate the effect of this omission on the different interaction energies. From the MP2/6-311++G** calculations, the interlayer Cl···O nonbonded interaction (X-ray, 304.5 pm) was determined to be 13.1 kJ mol^{-1}. This is a reasonably high intermolecular interaction energy and may help to explain the different orientation of the $CHCl_2$ group in the solid state compared to the gas phase. The intralayer H···O interactions (X-ray, 204.1 and 244.9 pm) were determined to correspond to an energy of 37.1 kJ mol^{-1}. This indicates that both the hydrogen bonds are also strong but the individual values cannot be resolved further. One of the hydrogen atoms involved in the bonding is the H of the $CHCl_2$ group, another indication as to why this particular group orientates itself in the way it does in the solid-state structure.

TABLE 3: Single Point Energy Calculations for Monomer and Two Different Dimers of $MeNHCOCHCl_2$ at the MP2/6-311++G and PW91PW91/6-311++G** Levels with Counterpoise Correction Calculations**

molecule/interaction	energy/ hartrees	interaction energy/ kJ mol^{-1} uncorrected[a]	interaction energy/ kJ mol^{-1} corrected[b]
MP2/6-311++G**/Cl···O		−18.9	−13.1
monomer	−1165.9291		
donor + ghost	−1165.9309		
acceptor + ghost	−1165.9314		
dimer	−2331.8655		
MP2/6-311++G**/H···O		−57.6	−37.1
donor + ghost	−1165.9320		
acceptor + ghost	−1165.9341		
dimer	−2331.8802		
PW91PW91/6-311++G**/Cl···O		−9.6	−6.9
monomer	−1167.6261		
donor + ghost	−1167.6264		
acceptor + ghost	−1167.6268		
dimer	−2335.2558		
PW91PW91/6-311++G**/H···O		−39.8	−36.4
donor + ghost	−1167.6267		
acceptor + ghost	−1167.6274		
dimer (H···O)	−2335.2673		

[a] E_{uncorr} = dimer − (2 × monomer) (uncorrected for basis set superposition error). [b] $E_{corr} = E_{uncorr}$ − (donor − monomer) − (acceptor − monomer) (corrected for basis set superposition error).

The DFT calculations (PW91PW91/6-311++G**) return a Cl···O interaction energy of 6.9 kJ mol^{-1} compared to the MP2 value of 13.1 kJ mol^{-1}. This indicates that some energy is "missing" from the DFT calculations of the nonbonded interactions. This missing energy is the effect of the dispersion forces, which, as mentioned previously, are neglected in the DFT calculations. The H···O calculated energy for two bonds is 36.4 kJ mol^{-1} compared to 37.1 kJ mol^{-1} calculated by the MP2 method. These energies are very similar, implying that the effects of the dispersion forces are negated by some other factor(s) for first-row atoms, but that they become important for interactions involving second-row atoms and beyond.

To ensure that the relative energies calculated by the two methods were consistent, the energy difference between the solid and gaseous structures was calculated at the MP2/6-311++G** and PW91PW91/6-311++G** levels (Table 3). The energy differences for the MP2 and DFT methods were 14.1 and 15.3 kJ mol^{-1}, respectively, with both returning the gaseous structure

TABLE 4: Geometric Parameters from Various Stages of Solid-State Plane Wave DFT Calculations[a,b]

parameter	X-ray	plane wave DFT	supercell (optimized)[c]	Cl···O interaction[d]	H···O interaction[d]
C═O	123.0	124.2	122.1	122.1	122.1
C−C	153.1	152.1	152.9	152.9	152.9
C−Cl	177.0	176.6	176.2	176.2	176.2
C−H(Cl_2)	99.0	109.1	109.1	109.1	109.1
N−C(H_3)	145.9	144.1	143.9	143.9	143.9
N−C(O)	131.5	133.1	135.3	135.3	135.3
N−H	87.0	103.6	101.7	101.7	103.6
O···H(1)	204.1	189.0			189.0
O···H(2)	244.9	240.6			240.6
Cl···O	304.5	311.7		311.7	
energy/molecule (hartree)		−2077.9193	−2077.3444	−2077.3985	−2077.8885

[a] Distances in pm. [b] ϕ(HCCO) always 180.0°. [c] Energy for single point supercell = −2077.3013 hartrees. [d] Single point energies.

as the more stable conformer. These energies are reasonably consistent and provide confidence for our previous assertions regarding interaction energies.

Solid-State Calculations. *Crystal Lattice Calculation.* The calculated structure, both geometry and unit cell vectors, agrees well with that obtained for the low-temperature crystal structure. The calculated unit-cell volume obtained is within 3.6 % of the crystal structure. There is good agreement between the calculated molecular geometry and that obtained experimentally in the low-temperature crystal structure. The largest difference between the values obtained for the non-hydrogen bond distances in the calculated and low-temperature crystal structures is 2 pm. The calculated distances for the nonbonded interactions do not match as well, with a difference of 15 pm for H···O(1) between calculated and observed values.

Supercell Calculations. The results from the two supercell calculations show that the geometry of the molecule changes little between the solid and gas phases in this orientation. The largest change is observed in the C═O bond length, which decreases by 2 pm from the crystal lattice to the supercell optimized calculation. This can be attributed to the fact that the oxygen atom is no longer involved in any intermolecular interactions, either to hydrogen or to chlorine atoms. The N−C(═O) bond distance is seen to increase in value from 133.1 to 135.3 pm between the calculation of the crystal lattice and supercell optimized calculation. This is also due to the destruction of the intermolecular interactions allowing the molecule to relax.

H···O and Cl···O Interactions. To study the H···O and Cl···O interactions, two of the four molecules were removed from the unit cell. Geometry optimizations were then not possible because the molecules would reorientate in a way that was not meaningful. The molecular geometries of the remaining molecules were therefore frozen and the energy recalculated. Relevant structural parameters from the above stages are given in Table 4, as well as those for the X-ray structure for comparison. The energy values obtained in these calculations are discussed later in this paper.

Gas-Phase Electron Diffraction Refinement. On the basis of the ab initio calculations described above, electron-diffraction refinements were carried out with use of a model of C_1 symmetry to describe the vapor. In accord with the calculations, the assumption of local C_{3v} symmetry for the methyl group was made.

The structure of $MeNHCOCHCl_2$ was finally defined in terms of 21 independent geometric parameters, comprising 7 bond lengths and differences, 10 bond angles and differences, and 4 torsion parameters [Table 2; atom numbering shown in Figure 1]. See the Supporting Information for the parameter definitions.

TABLE 5: Comparison of Geometrical Parameters for *N*-Methyldichloroacetamide from the X-ray Diffraction, Gas Electron Diffraction, and Theoretical Structures[a]

parameter	MP2/6-311++G**	GED	X-ray
C(2)−N(3)	145.4	146.8(3)	145.8(4)
N(3)−C(7)	135.1	136.9(3)	131.5(3)
C(7)═O(8)	122.4	124.7(3)	123.0(3)
C(7)−C(9)	153.3	153.7(3)	153.1(4)
C−Cl(11)	177.5	178.4(2)	177.0(2)
C−Cl(12)	177.8	178.4(2)	177.0(2)
C(2)−N(3)-C(7)	120.3	118.7(10)	121.7(2)
N(3)−C(7)═O(8)	124.4	123.0(4)	125.0(2)
N(3)−C(7)-C(9)	115.9	118.0(6)	114.5(2)
O(8)═C(7)−C(9)	119.4	119.0(6)	120.5(2)
C(7)−C(9)−Cl(11)	109.9	110.7(5)	108.7(1)
C(7)−C(9)−Cl(12)	112.0	114.7(5)	108.7(1)
Cl(11)−C(9)−Cl(12)	111.3	110.7(2)	110.5(1)
C(2)−N(3)−C(7)═O(8)	3.1	2.0(24)	0.0
O(8)═C(7)−C(9)−H(10)	−13.1	−31.8(22)	180.0

[a] See Figure 1 for atom numbering.

The starting parameters for the r_{h1} refinement[33] were taken from the theoretical geometry optimized at the MP2/6-311++G** level. Theoretical (MP2/6-311++G**) Cartesian force fields were obtained and converted into force fields described by a set of symmetry coordinates with use of the SHRINK program.[33] All geometric parameters were then refined.

In total all 21 geometric parameters and 16 groups of vibrational amplitudes were refined. Flexible restraints were employed during the refinement with use of the SARACEN method.[34] Altogether, 14 geometric and 9 amplitude restraints were employed. These are listed in Table 5.

In the final refinement, R factors were $R_G = 0.041$ and $R_D = 0.048$. The radial distribution curve and the molecular scattering intensity curves are shown in Figures 6 and 7, respectively. Final refined parameters are listed in Table 2, interatomic distances and the corresponding amplitudes of vibration in Table S4 (Supporting Information), and the least-squares correlation matrix in Table S5 (Supporting Information). Experimental coordinates from the GED analysis are given in Table S6 (Supporting Information). Figure 1 shows a perspective view of $MeNHCOCHCl_2$ in the optimum refinement of the GED data, as well as a view down the (O−)C−N bond

X-ray Crystallography. Solid-state structural analysis of $MeNHCOCHCl_2$ was carried out with low-temperature single-crystal X-ray diffraction at 233 K. The solid structure was found to possess the orthorhombic space group *Pnma* with four molecules per unit cell. The structure was solved by direct methods[35] and all non-hydrogen atoms were treated as aniso-

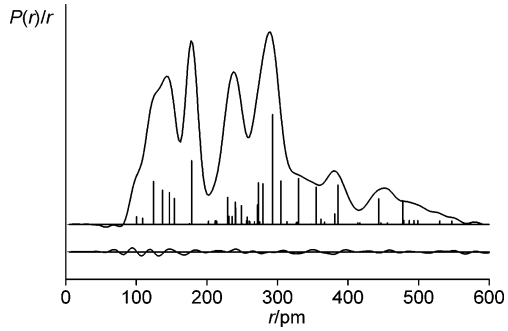

Figure 6. Experimental and difference (experimental − theoretical) radial-distribution curves, $P(r)/r$, for $MeNHCOCHCl_2$. Before Fourier inversion the data were multiplied by $s\exp(-0.00002s^2)/(Z_{Cl} - f_{Cl})/(Z_C - f_C)$.

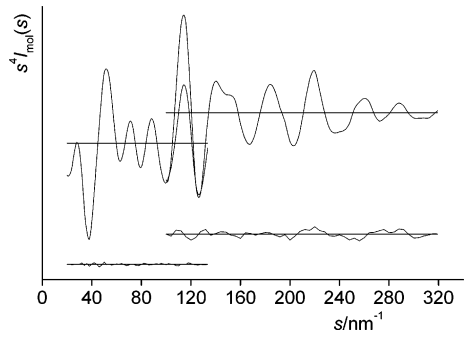

Figure 7. Experimental and final weighted difference (experimental − theoretical) molecular-scattering intensities for $MeNHCOCHCl_2$.

tropic. In the solid state $MeNHCOCHCl_2$ adopts a planar heavy-atom structure with ϕ(HCCO) = 180°. The atoms C(2), N(3), C(7), O(8), and C(9) lie on a mirror plane that relates Cl(11) and Cl(12). The methyl group was modeled as two groups related by a 180° rotation at equal occupancy. The crystal structure is the same as shown in Figure 4. The geometrical parameters determined by the X-ray crystallographic study of *N*-methyldichloroacetamide are listed in Table 5, along with the equivalent parameters from the gas electron diffraction and ab initio study.

Discussion

The structural properties of *N*-methyldichloroacetamide have been investigated in the gas phase by gas-phase electron diffraction and ab initio methods, in the fluid phase by ab initio solvent-inclusion methods, and in the solid phase by X-ray crystallography, ab initio, and plane-wave density functional methods.

In general, the experimental gas-phase and theoretical structures agree well with each other. Theoretical bond lengths were generally found to be within 1−2 pm of the experimental values, and the bond angles were also within 1−2° of the experimental values. The main difference between the structures occurs in the HCCO bond torsion. The value of ϕ(HCCO) is calculated to be −13.1° for the free molecule at the MP2/6-311++G** level, whereas a value of −31.8(22)° is returned by the GED experiment. However, if the structure is constrained to the value calculated at the MP2/6-311++G** level, the *R* factor rises significantly (0.105 compared to 0.041), indicating that the goodness of fit for the experimental data has deteriorated significantly with the imposition of the ab initio value. Given the large variation of this torsion angle, by ∼15°, during the calculations, this difference between the experimental and ab initio value for this parameter is not surprising. Examination of the correlation matrix (Table S5) indicates that this parameter is not heavily correlated with any others, and during the refinement procedure the parameter was very stable, barely changing from the final reported value on refinement of other parameters. Another test was to constrain the HCCO torsion angle to the value obtained from the GED study and recalculate the molecular structure at the MP2/6-311++G** level to evaluate the energy difference between the two. This energy difference was found to be just 1.2 kJ mol^{-1}. Figure 5 shows the energy differences for the torsional variation at the B3LYP level. It can be seen that the potential is very flat for ϕ(HCCO) between −20° (340°) and 20°. Both these pieces of evidence indicate that it is relatively easy for the molecule to deviate from the equilibrium structure as calculated ab initio to the GED structure, which *is* corrected for the effects of vibrations at the temperature of the experiment.

Although parameters determined in the gaseous and solid phases are not directly comparable because of the differences in diffraction techniques, most of the X-ray crystallographic parameters agree well with those in the gas phase. However, there are significant differences between the N(3)−C(7) bond distances [GED, 136.9(3) pm; X-ray, 131.5(3) pm], and the N(3)−C(7)−C(9) and C(7)−C(9)−Cl(11/12) bond angles. GED determines the N−C−C bond angle to be 118.0(6)°, significantly larger than the value of 114.5(2)° for the crystal, while the C−C−Cl(12) bond angle was found to be 114.7(5)° by GED and only 108.7(1) by X-ray crystallography.

The shortening of the N−C bond has been observed previously for other acetamides.[36,37] In acetamide,[36] the C−N bond was determined to be 138.0(4) pm in the gas phase compared to 133.4(17) pm in the crystal structure.[38] In *N*-methylacetamide,[37] the gaseous C−N bond length was found to be 138.6 pm, nearly 10 pm longer than the solid-state value of 129.0 pm.[39] The shortening of these bonds in all cases can be attributed to the intermolecular hydrogen bonding in the solid structures. In the cases of acetamide and *N*-methylacetamide, the C═O bond length was also consistently shorter in the gas-phase structures than in the solid-phase ones. For example, in acetamide the gaseous C═O bond was 122.0(3) pm compared to 126.0(11) pm in the solid state. The difference was not so dramatic in *N*-methylacetamide (gas, 122.5 pm; solid, 123.6 pm), while in *N*-methyldichloroacetamide the C═O bond length is actually determined to be longer in the gas phase than in the solid phase [gas, 124.7(3) pm; solid, 123.0(3) pm]. The gaseous C═O bond length is much longer in *N*-methyldichloroacetamide than in *N*-methylacetamide and acetamide [124.7(3) pm cf. 122.5 and 122.0(3) pm]. This can be attributed to the electron-withdrawing effect of the two chlorine atoms on the $CHCl_2$ group adjacent to the C═O bond, weakening it and making it longer. The solid-phase C═O bond length is similar to that in *N*-methylacetamide, while both these are much less than that in acetamide.

The torsion angle ϕ(HCCO) in the gaseous structure was also investigated in a solvent field at the B3LYP/6-31G** level to gauge the effects of tetrachloromethane and dimethyl sulfoxide (DMSO) on the conformation of the molecule. When no solvent is present, there is a definite maximum in the curve at ϕ(HCCO) ∼ 180°, confirming that this structure is not real in the gas phase. Using CCl_4 as a solvent results in a very broad maximum at ϕ(HCCO) ∼ 150° to 200°, implying that CCl_4 does not change the preferred conformation of the molecule, or predispose it to form the observed solid-state conformation about the C−C bond. However, using DMSO as a solvent does result in a minimum at ϕ(HCCO) ∼ 180°. This minimum is significantly higher in

energy than that observed for ϕ(HCCO) $\sim$ 20° (6.9 kJ mol^{-1}), corresponding to a 94.2:5.8 mixture of conformers at room temperature and a 97.6:2.4 mixture at 223 K (the temperature at which the crystal was formed). Of course, the conformation adopted in the crystal depends on the total energy of the system, which depends on the sum of all interactions. Nevertheless, the calculations do show that a second conformation, with ϕ(HCCO) = 180°, is possible.

Further investigation of the solid-state structure was undertaken with ab initio molecular orbital and plane-wave DFT methods to investigate whether there are solid-state interactions that would favor molecular crystal formation with ϕ(HCCO) = 180° (as opposed to the gaseous ϕ(HCCO) = −30°). These intermolecular bonds should ideally involve the hydrogen and chlorine atoms of the $CHCl_2$ group to help explain the conformation observed. Examination of the crystal structure reveals possible interlayer Cl···O bonding (Figure 2a) involving chlorine from the $CHCl_2$ group, and two possible intralayer H···O bonds (Figure 2b) involving the hydrogen of the $CHCl_2$ group and the amide hydrogen, both with the carbonyl oxygen.

Two different dimers were chosen to describe the interactions to be investigated ab initio, using ab initio MO single-point energy calculations on the crystal coordinates. One dimer described the single Cl···O interaction while the other described the two H···O bonds, although it is impossible to resolve them further. Both MP2 and DFT methods (MP2/6-311++G**/PW91PW91/6-311++G**) were used to analyze any differences between the two methods, especially for the Cl···O interactions. Although the Cl···O interaction may be classically regarded as repulsive, it has been previously observed that weak Cl···O interactions may be important in stabilizing a structure. For example, the solid-state structure of oxalyl chloride[40] is anti, with weak Cl···O interactions, while the gaseous structure was found to be a mixture of anti and gauche conformers in an approximate 50:50 mixture (varying with temperature).[41] Therefore, although not contributing much energy, these interactions can be important and cannot be ignored altogether from the theoretical study. From Table 3 it can be seen that the interaction energy for the Cl···O bond was 13.1 kJ mol^{-1} for MP2 and 6.9 kJ mol^{-1} for DFT. For the H···O interactions, the energy was very similar from both MP2 and DFT methods (37.1 and 36.4 kJ mol^{-1}, respectively). The substantial difference between the MP2 and DFT methods for the Cl···O interaction can be attributed to the lack of modeling of dispersion forces by DFT. It is anticipated that a significant proportion of the Cl···O bond will be van der Waals in nature, which is not modeled in current DFT functionals. The pure ab initio method (in this case MP2) gives a more rigorous approximation of the forces, and so the interaction energy is higher. This is especially significant for interactions involving atoms in the second row and higher.

The solid-state interactions were also investigated under periodic boundary conditions by PW-DFT and compared to the energies obtained from the ab initio MO investigation. These calculations are especially interesting as they involve optimizing the structure under periodic conditions, where the surrounding molecules influence the molecular structure. In this case the Cl···O interaction energy was calculated to be just 2.4 kJ mol^{-1}, while the H···O interactions were predicted to be 46.5 kJ mol^{-1}. Comparing with the ab initio MO values (PW91PW91, 6.9 and 36.4 kJ mol^{-1}; MP2, 13.1 and 37.1 kJ mol^{-1}) it appears that under periodic conditions the H···O interactions have much more influence on the structure than the Cl···O interaction. Closer observation of the solid-state structure reveals that the H···O interactions form a chain across the molecules, with each interaction further stabilizing the next one. These synergistic interactions help to stabilize the overall solid-state structure, with the energy gained from the solid-state H···O interactions (between 36 and 46 kJ mol^{-1}) overcoming the energy lost by rotating the $CHCl_2$ group from ϕ(HCCO) = −31° to ϕ(HCCO) = 180° upon crystallization ($\sim$15 kJ mol^{-1}). We believe that this is the reason for the dramatic conformational change observed on going from that gas to the solid phase. The increase in energy of hydrogen bonding by $\sim$10 kJ mol^{-1} from the dimer system to the periodic system has been observed previously for urea.[42] In this case, Dannenberg et al. demonstrated that as the urea dimer was extended to form an infinite one-dimensional chain, the strength of intermolecular interaction increased by almost 10 kJ mol^{-1}.

Other molecules containing the dichloroacetamido moiety have also been investigated to examine the correlation between the HCCO torsion angle and intermolecular hydrogen bonding in the solid phase. A search of the Cambridge Structural Database (CSD)[43,44] reveals 14 structures with the $NHCOCHCl_2$ moiety, 12 of which possess the torsion ϕ(HCCO) $\sim$ 180°. Close examination of the crystal structures of dichloroacetylaminoisobutyric acid[45] and chloramphenicol[46] both reveal hydrogen bonding between the carbonyl oxygen on one molecule and the N−H and $CHCl_2$ hydrogen atoms on an adjacent molecule. Both these structures yield ϕ(HCCO) $\sim$ 180°. It is observed that for the 12 structures with ϕ(HCCO) $\sim$ 180°, hydrogen bonding between both the H of the $CHCl_2$ group and the H of the amido group to the adjacent carbonyl is always present. Thiamphenicol[47] is a close relative of chloramphenicol, simply replacing the NO_2 group with a SO_2CH_3 group. In this case, hydrogen bonding is also observed at the carbonyl oxygen and $CHCl_2$ hydrogen, but involving one of the S═O bonds and the sulfonyl methyl group. In this case, ϕ(HCCO) is $\sim$0°, which serves to facilitate the observed bonding. Thus it appears that the $CHCl_2$ group orientates itself in the solid state to optimize hydrogen bonding, and hence stabilization of the crystal structure. In the one remaining structure from the CSD, no bonding between the $CHCl_2$ group and any other group is present, and in this case ϕ(HCCO) was observed to be −45°, close to that observed in our gas-phase structure.

Conclusions

The structure of *N*-methyldichloroacetamide has been elucidated in the gas and solid phases. The gas-phase structure was found to be that with ϕ(HCCO) = −31.8(22)°, similar to the most energetically favorable conformer by ab initio calculations. The solid state was found to consist of a conformer with ϕ(HCCO) = 180.0°. This was also found to be energetically favorable, by further theoretical investigations of the crystal structure, because of solid-state interactions that are not possible for the gaseous conformation. The combined use of gas- and solid-phase experimental and theoretical techniques, including the relatively new plane-wave DFT method, has facilitated the structural investigation of this apparently straightforward but nevertheless fascinating molecule.

Acknowledgment. We thank the U.K. Computational Chemistry Facility (admin: Department of Chemistry, King's College London, Strand, London WC2R 2LS) for the computing time on Columbus and Dr. Svein Samdal (University of Oslo) for helpful discussions. C.A.M. is grateful to the Royal Society for the award of a University Research Fellowship.

Supporting Information Available: Parameter descriptions for the GED model of $MeNHCOCHCl_2$ (text); nozzle-to-plate

distances (mm), weighting functions (nm^{-1}), correlation parameters, scale factors, and electron wavelengths (pm) used in the gas electron diffraction study of $MeNHCOCHCl_2$; X-ray crystal structure data collection, processing, solution, and refinement for $MeNHCOCHCl_2$; molecular geometry of the lowest energy (*syn0*) C_1 structure of $MeNHCOCHCl_2$ at the HF/6-31G*, MP2/6-31G*, MP2/6-311G*, and MP2/6-311+G* levels of theory; interatomic distances (*r*/pm) and amplitudes of vibration (*u*/pm) for the restrained GED structure of $MeNHCOCHCl_2$; least-squares correlation matrix ($\times 100$) for $MeNHCOCHCl_2$; experimental GED coordinates for $MeNHCOCHCl_2$ (all tables). This material is available free of charge via the Internet at http://pubs.acs.org.

References and Notes

(1) Samdal, S.; Seip, R. *J. Mol. Struct.* **1997**, *413*−*414*, 423.

(2) Gundersen, S.; Novikov, V. P.; Samdal, S.; Seip, R.; Shorokov, D. J.; Sipachev, V. A. *J. Mol. Struct.* **1999**, *485*−*486*, 97.

(3) Gundersen, S.; Samdal, S.; Seip, R.; Shorokov, D. J. *J. Mol. Struct.* **1999**, *477*, 225.

(4) Fausto, R.; Teixeira-Dias, J. J. C. *J. Mol. Struct.* **1986**, *144*, 225.

(5) Fausto, R.; Teixeira-Dias, J. J. C. *J. Mol. Struct.* **1986**, *144*, 241.

(6) Tormena, C. F.; Amadeu, N. S.; Rittner, R.; Abraham, R. J. *J. Chem. Soc., Perkin Trans. 2* **2002**, 773.

(7) Kulbida, A.; Fausto, R. *J. Chem. Soc., Faraday Trans.* **1993**, *89*, 4257.

(8) Litvinov, O. A.; Zuev, M. B.; Naumov, V. A.; Volden, H. V.; Hagen, K. *J. Phys. Chem.* **1993**, *97*, 10674.

(9) Shen, Q.; Hilderbrandt, R.; Hagen, K. *J. Mol. Struct.* **1980**, *71*, 161.

(10) Ginzburg, I. M. *Zh. Obsch. Khim.* **1983**, *53*, 2563.

(11) Thomas, E. W. Manuscript in preparation.

(12) Liler, M. *J. Chem. Soc. B* **1969**, 385. Molday, R. S.; Kallen, R. G. *J. Am. Chem. Soc.* **1972**, *94*, 6739.

(13) Frisch, M. J.; Trucks, G. W.; Schlegel, H. B.; Scuseria, G. E.; Robb, M. A.; Cheeseman, J. R.; Zakrzewski, V. G.; Montgomery, J. A., Jr.; Stratmann, R. E.; Burant, J. C.; Dapprich, S.; Millam, J. M.; Daniels, A. D.; Kudin, K. N.; Strain, M. C.; Farkas, O.; Tomasi, J.; Barone, V.; Cossi, M.; Cammi, R.; Mennucci, B.; Pomelli, C.; Adamo, C.; Clifford, S.; Ochterski, J.; Petersson, G. A.; Ayala, P. Y.; Cui, Q.; Morokuma, K.; Malick, D. K.; Rabuck, A. D.; Raghavachari, K.; Foresman, J. B.; Cioslowski, J.; Ortiz, J. V.; Baboul, A. G.; Stefanov, B. B.; Liu, G.; Liashenko, A.; Piskorz, P.; Komaromi, I.; Gomperts, R.; Martin, R. L.; Fox, D. J.; Keith, T.; Al-Laham, M. A.; Peng, C. Y.; Nanayakkara, A.; Gonzalez, C.; Challacombe, M.; Gill, P. M. W.; Johnson, B.; Chen, W.; Wong, M. W.; Andres, J. L.; Gonzalez, C.; Head-Gordon, M.; Replogle, E. S.; Pople, J. A. *Gaussian 98*, Revision A.7; Gaussian, Inc.: Pittsburgh, PA, 1998.

(14) Segall, M. D.; Lindan, P. L. D.; Probert, M. J.; Pickard, C. J.; Hasnip, P. J.; Clark, S. J.; Payne, M. C. *J. Phys, Condens. Matter* **2002**, *14* (11), 2717−2743.

(15) Binkley, J. S.; Pople, J. A.; Hehre, W. J. *J. Am. Chem. Soc.* **1980**, *102*, 939.

(16) Gordon, M. S.; Binkley, J. S.; Pople, J. A.; Pietro, W. J.; Hehre, W. J. *J. Am. Chem. Soc.* **1982**, *104*, 2797.

(17) Pietro, W. J.; Francl, M. M.; Hehre, W. J.; DeFrees, D. J.; Pople, J. A.; Binkley, J. S. *J. Am. Chem. Soc.* **1982**, *104*, 5039.

(18) Hehre, W. J.; Ditchfield, R.; Pople, J. A. *J. Chem. Phys.* **1972**, *56*, 2257.

(19) Hariharan, P. C.; Pople, J. A. *Theor. Chim. Acta* **1973**, *28*, 213.

(20) Gordon, M. S. *Chem. Phys. Lett.* **1980**, *76*, 163.

(21) McLean, A. D.; Chandler, G. S. *J. Chem. Phys.* **1980**, *72*, 5639.

(22) Krishnan, R.; Binkley, J. S.; Seeger, R.; Pople, J. A. *J. Chem. Phys.* **1980**, *72*, 650.

(23) (a) Becke, A. D. *J. Chem. Phys.* **1993**, *98*, 5648. (b) Lee, C.; Yang, W.; Parr, R. G. *Phys. Rev. B* **1988**, *37*, 785.

(24) (a) Wong, M. W.; Frisch, M. J.; Wiberg, K. B. *J. Am. Chem. Soc.* **1991**, *113*, 4776. (b) Wong, M. W.; Wiberg, K. B.; Frisch, M. J. *J. Am. Chem. Soc.* **1992**, *114*, 523. (c) Wong, M. W.; Wiberg, K. B.; Frisch, M. J. *J. Am. Chem. Soc.* **1992**, *114*, 1645.

(25) van Duijneveldt, F. B.; van Duijneveldt-van de Rijdt, J. G. C. M.; van Lenthe, J. H. *Chem. Rev.* **1994**, *94*, 1873.

(26) Perdew, J. P.; Burke, K.; Ernzerhof, M. *Phys. Rev. Lett.* **1997**, *77*, 3865.

(27) Monkhurst, H. J.; Pack, J. D. *Phys. Rev. B* **1976**, *13*, 5188.

(28) Huntley, C. M.; Laurenson, G. S.; Rankin, D. W. H. *J. Chem. Soc., Dalton Trans.* **1980**, 954.

(29) Lewis, J. R.; Brain, P. T.; Rankin, D. W. H. *Spectrum* **1997**, *15*, 7.

(30) Cradock, S.; Koprowski, J.; Rankin, D. W. H. *J. Mol. Struct.* **1981**, *77*, 113.

(31) Boyd, A. S. F.; Laurenson, G. S.; Rankin, D. W. H. *J. Mol. Struct.* **1981**, *71*, 217.

(32) Ross, A. W.; Fink, M.; Hilderbrandt, R. *International Tables for Crystallography*; Wilson, A. J. C., Ed.; Kluwer Academic Publishers: Dordrecht, The Netherlands, , 1992; Vol. C, p 245.

(33) Sipachev, V. A. *J. Mol. Struct. (THEOCHEM)* **1985**, *121*, 143.

(34) Brain, P. T.; Morrison, C. A.; Parsons, S.; Rankin, D. W. H. *J. Chem. Soc., Dalton Trans.* **1996**, 4589. Blake, A. J.; Brain, P. T.; McNab, H.; Miller, J.; Morrison, C. A.; Parsons, S.; Rankin, D. W. H.; Robertson, H. E.; Smart, B. A. *J. Phys. Chem.* **1996**, *100*, 12280.

(35) Sheldrick, G. M. *Acta Crystallogr.* **1990**, *A46*, 467.

(36) Kitano, M.; Kuchitsu, K. *Bull. Chem. Soc. Jpn.* **1973**, *46*, 3048.

(37) Kitano, M.; Fukuyama, T.; Kuchitsu, K. *Bull. Chem. Soc. Jpn.* **1973**, *46*, 384.

(38) Hamilton, W. C. *Acta Crystallogr.* **1965**, *18*, 866

(39) Katz, J. L.; Post, B. *Acta Crystallogr.* **1960**, *13*, 624.

(40) Groth, P.; Hassel, O. *Acta Chem. Scand.* **1962**, *16*, 2311.

(41) Hagen, K.; Hedberg, K. *J. Am. Chem. Soc.* **1973**, *95*, 1003.

(42) Masunov, A.; Dannenberg, J. J. *J. Phys. Chem. B* **2000**, *104*, 806.

(43) CONQUEST, Cambridge Crystallographic Data Centre, Cambridge, 2001.

(44) CSD Version 5.34: Allen, F. H.; Kennard, O. *Chem. Design Autom. News* **1993**, *8*, 31.

(45) Valle, G.; Bonora, G. M.; Toniolo, C. *Gazz. Chim. Ital.* **1984**, *114*, 481.

(46) Chatterjee, C.; Dattagupta, J. K.; Saha, N. N.; Saenger, W.; Muller, K. *J. Cryst. Mol. Struct.* **1979**, *9*, 295.

(47) Ghosh, M.; Basak, A. K.; Mazumdar, S. K.; Párkányi, L.; Kálmán, A. *Acta Crystallogr.* **1987**, *C43*, 1552.